

Cite this: *Phys. Chem. Chem. Phys.*, 2011, **13**, 2690–2700

www.rsc.org/pccp

PAPER

Effect of substituents on redox, spectroscopic and structural properties of conjugated diaryltetrazines—a combined experimental and theoretical study†

Ewa Kurach,^a David Djurado,^b Jan Rimarčík,^c Aleksandra Kornet,^a Marek Wlostowski,^a Vladimir Lukeš,^c Jacques Pécaut,^d Malgorzata Zagorska*^a and Adam Pron*^b

Received 19th August 2010, Accepted 11th November 2010

DOI: 10.1039/c0cp01553a

Two series of new soluble conjugated compounds containing tetrazine central ring have been synthesized. The three-ring compounds have been synthesized by the reaction of aryl cyanide (where aryl = thienyl, alkylthienyl, phenyl or pyridyl) with hydrazine followed by oxidation of the intermediate product with diethyl azodicarboxylate. The five-ring compounds have been prepared using two pathways: (i) reaction of 5-cyano-2,2'-bithiophene (or its alkyl derivative) with hydrazine; (ii) *via* Suzuki or Stille coupling of 3,6-bis(5-bromo-2-thienyl)-1,2,4,5-tetrazine with a stannyl or boronate derivative of alkylthiophene. UV-vis spectroscopic properties of the synthesized compounds are strongly dependent on the nature of the aryl group, the position of the solubilizing substituent and the length of the molecule, showing the highest bathochromic shift ($\lambda_{\text{max}} > 440$ nm) for five-ring compounds with alkyl groups attached to C $_{\alpha}$ carbon in the terminal thienyl ring. An excellent linear correlation has been found for spectroscopically determined and theoretically calculated (TD-B3LYP/6-31G*) excitation energies. With the exception of dipyridyl derivative, the calculated lowest unoccupied molecular orbital (LUMO) level of the investigated molecules changes within a narrow range (from -2.63 to -2.41 eV), in line with the electrochemical data, which show a reversible reduction process with the redox potential varying from -1.23 V to -1.33 V (*vs.* Fc/Fc⁺). The electrochemically determined positions of the LUMO levels are consistently lower by 0.9 to 1.2 eV with respect to the calculated ones. All molecules readily crystallize. Single crystal studies of 3,6-bis(2,2'-bithien-5-yl)-1,2,4,5-tetrazine show that it crystallizes in a *P2₁/c* space group whose structural arrangement is not very favorable to the charge carriers flow within the crystal. Powder diffraction studies of other derivatives have shown that their structural organization is sensitive to the position of the solubilizing substituent. In particular, the presence of alkyl groups attached to C $_{\alpha}$ carbon in the terminal thienyl ring promotes the formation of a lamellar-type supramolecular organization.

^a Faculty of Chemistry, Warsaw University of Technology, Noakowskiego 3, 00 664 Warszawa, Poland.

E-mail: zagorska@ch.pw.edu.pl

^b INAC/SPRAM (UMR 5819 CEA-CNRS-Univ. J. Fourier-Grenoble 1), Laboratoire d'Electronique Moléculaire Organique et Hybride, 17 Rue des Martyrs, 38054 Grenoble Cedex 9, France.

E-mail: adam.pron@cea.fr

^c Institute of Physical Chemistry and Chemical Physics, Slovak University of Technology in Bratislava, SK-81 237 Bratislava, Slovakia

^d INAC/SCIB CEA Grenoble, 17 Rue des Martyrs, 38054 Grenoble Cedex 9, France

† Electronic supplementary information (ESI) available: Synthesis of all molecules. The depiction of bonds forming the main conjugation chain. Schematic representation of the relative energy between experimental and B3LYP HOMOs and LUMOs for studied molecules. The calculated TD-B3LYP optical transitions for studied molecules. CCDC reference number 774463. For ESI and crystallographic data in CIF or other electronic format see DOI: 10.1039/c0cp01553a

Introduction

Conjugated molecules and macromolecules play an important role in modern materials science. They can be used as semiconductors in organic electronics^{1,2} or optoelectronics³ components of electrochemical sensors^{4,5} advanced electrode materials⁶ and other types of functional materials. All these applications require designing molecules (macromolecules) with precisely tuned physicochemical properties. Control of their HOMO (Highest Occupied Molecular Orbital) and LUMO (Lowest Unoccupied Molecular Orbital) level positions is especially important in this respect since to a first approximation they govern the electronic, spectroscopic and redox properties of a given molecule. As a general rule, introduction of an electron accepting group to a conjugated molecule (macromolecule)

lowers its LUMO level whereas the presence of an electron donating unit raises the HOMO level. Using the building block strategy several low band gap, donor–acceptor type conjugated compounds were prepared, suitable for photovoltaic and other applications.⁷ Similarly, appropriate functionalization of conjugated molecules (macromolecules) with electron accepting groups resulted in the preparation of several organic semiconductors with low lying LUMO levels suitable for fabrication of n-channel organic field effect transistors (OFETs) operating in air.⁸ In this context bis-substituted tetrazines, containing aryl substituents, can be considered as donor–acceptor–donor (DAD) molecules in which the central unit is strongly electron deficient. They can serve as building blocks for new low band gap conjugated polymers⁹ or, in some cases, as macromonomers, undergoing electrochemical polymerization.¹⁰ Due to their low lying LUMO level they undergo reversible electrochemical reduction at much higher potentials as compared to the reduction of their thiophene homooligomers.¹¹ This makes them promising candidates for the use in electrochromic devices and, since some of them are fluorescent, also in electrofluorochromic ones.¹² Synthetic and physical chemistries of tetrazine derivatives have recently been profoundly discussed in two exhaustive review papers.^{13,14}

Unsubstituted DAD conjugated molecules containing thiophene and tetrazine units are difficult to process due to their limited solubility. It can be significantly improved by synthesizing their derivatives containing long alkyl substituents, similarly as in the case of oligo- and poly(thiophenes).¹⁵ However, this approach must be exploited with caution since essentially all physico-chemical properties of this family of organic semiconductors depend on their regiochemistry—two regioisomers may exhibit strikingly different electronic and optical properties.¹⁶ Moreover, the presence of long alkyl groups may have a profound effect on the supramolecular organization of these compounds, frequently facilitating their self-assembly through interdigitation.¹⁷

The main goal of this paper was to synthesize new regiochemically well defined DAD-type electroactive molecules of improved processability and tunable HOMO–LUMO levels, which can be of potential use in organic electrochemical, electronic and optoelectronic devices. The relationships between their optical, electrochemical properties and molecular structure have been studied at a Density Functional Theory (DFT) level.

Experimental

Procedures for the preparation of compounds studied in this research are described in detail in ESI† together with their spectroscopic (NMR, FTIR) and elemental analysis data.

UV-vis spectra of the synthesized compounds dissolved in methylene chloride were recorded on a Varian Cary 5000 spectrometer. Cyclic voltammetry investigations of the synthesized diaryltetrazines were carried out using an Autolab potentiostat (Eco Chemie). The studied compounds were dissolved in 0.1 M methylene chloride solution of Bu₄NBF₄. The measurements were performed using a platinum working

electrode of a surface area of 3 mm², a platinum wire counter electrode and an Ag/0.1 M AgNO₃ acetonitrile reference electrode. The potential of the reference vs. Fc/Fc⁺ redox couple was checked at the end of each experiment. X-Ray powder diffraction investigations were carried out on an X-Pert Pro MPD Philips diffractometer (cobalt K_{α1} radiation; $\lambda = 1.789 \text{ \AA}$) using Bragg–Brentano ($\theta/2\theta$) reflection geometry. The detector was moved by 2θ steps of 0.02° and the counting time was at least 10 s per step. The divergence slit was automatically adjusted giving a 10 mm irradiated length. In the case of single crystals study, the X-ray Crystallography Diffraction data were taken at 150 K using an Oxford-Diffraction XCallibur S Kappa geometry diffractometer (MoK α radiation, graphite monochromator, $\lambda = 0.71073 \text{ \AA}$). The cell parameters were obtained with intensities detected on three batches of 5 frames. For three settings of ϕ and θ , 277 narrow data were collected for 1° increments in ω with a 20 s exposure time. Unique intensities detected on all frames using the Oxford-diffraction Red program were used to refine the values of cell parameters. The hydrogen atoms were all fixed in ideal positions. 10 794 reflections comprising 3751 independent ones were collected. The obtained final R indices were $R1 = 0.037$ and $wR2 = 0.0555$.

Theoretical calculations

The electronic ground state geometries of studied systems were optimized using Density Functional Theory (DFT)¹⁸ based on the Becke's three parameter hybrid functional using the Lee, Yang and Parr correlation functional for Gaussian (B3LYP).¹⁹ Based on the optimized geometries, the vertical transition energies and oscillator strengths between the initial and final states were computed by Time dependent version (TD-) of DFT method.²⁰ The 6-31G* basis set has been used^{21,22} and the calculations were done using the Gaussian 03 program package.²³ The energy cut-off was of $10^{-3} \text{ kcal mol}^{-1}$ and the final root mean square energy gradient was under $0.01 \text{ kcal mol}^{-1} \text{ \AA}^{-1}$. The obtained optimal structures were checked by normal mode analysis (no imaginary frequencies for all optimal geometries). The numerical integration of the used functional was performed using the fine integration grid which parameters were set as default. Due to the extreme computational requirements, our theoretical model was restricted to the single molecule without taking any solvent nor temperature effects into account as a standard simplification used in quantum chemical studies.

Results and discussion

Synthesis

Two series of compounds were synthesized, namely tetrazines with aryl and biaryl substituents. Their chemical formulae are depicted in Chart 1.

For simplicity, in the subsequent text compounds **1–5** will be termed “three-rings” and compounds **6–9**—“five-rings”. **4**, **5**, **7**, **8**, **8a**, **9** have not been reported in the literature, the remaining compounds were synthesized and studied for comparative reasons.

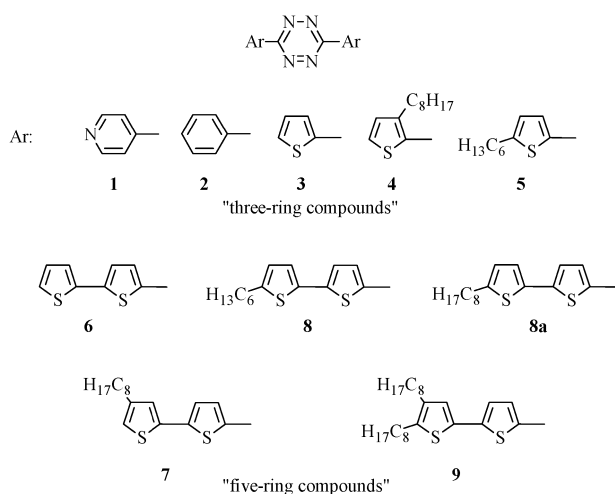
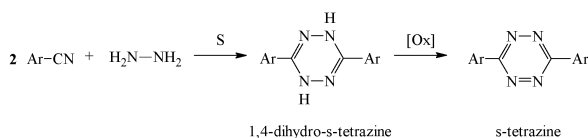


Chart 1 Tetrazine derivatives synthesized and studied in this research.



Scheme 1 Pinner's type synthesis of diaryltetrazines.

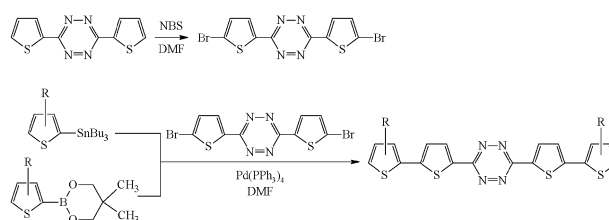
Scheme 2 Synthetic route to alkyl substituted five-ring compounds.

Three-rings were prepared in high yields using a modification of Pinner's procedure, in its simplest version shown in Scheme 1.

The synthesis pathway involves the reaction of aryl cyanide and hydrazine to yield 1,4-dihydro-tetrazine—an intermediate product—which is then converted to the desired diaryltetrazine using a mild oxidant as for example isoamyl nitrite as recommended in ref. 24. In our syntheses we have however used a different oxidizing agent, namely diethyl azodicarboxylate which assures clean oxidation and high yield of the reaction.²⁵

The same synthetic strategy can be applied to five-ring compounds already exploited by Audebert *et al.*¹⁰ It was tested by us in the preparation of **6** and **8** as one of the applied methods. This reaction pathway is however inconvenient for the derivatives containing alkyl groups because it involves a synthesis of cyano- and alkyl-substituted bithiophene which requires several steps, as shown in Scheme 2.

One may however ascertain that dibromo derivative of **3** can serve as a building block for the synthesis of a whole series of five-ring compounds *via* Stille or Suzuki coupling (see Scheme 3). This strategy not only significantly facilitates



Scheme 3 Preparation of five-ring compounds *via* Stille or Suzuki coupling of dibromo-derivative of **3**.

the synthetic route but also results in better yields as checked in the synthesis of **6** and **8** (see ESI†).

Unsubstituted as well as substituted three-rings (**1–5**) readily dissolve in chlorinated solvents. An unsubstituted five-ring compound (**6**) is less soluble, however, the introduction of long alkyl chains improves its solubility, most significantly in the case of **9**.

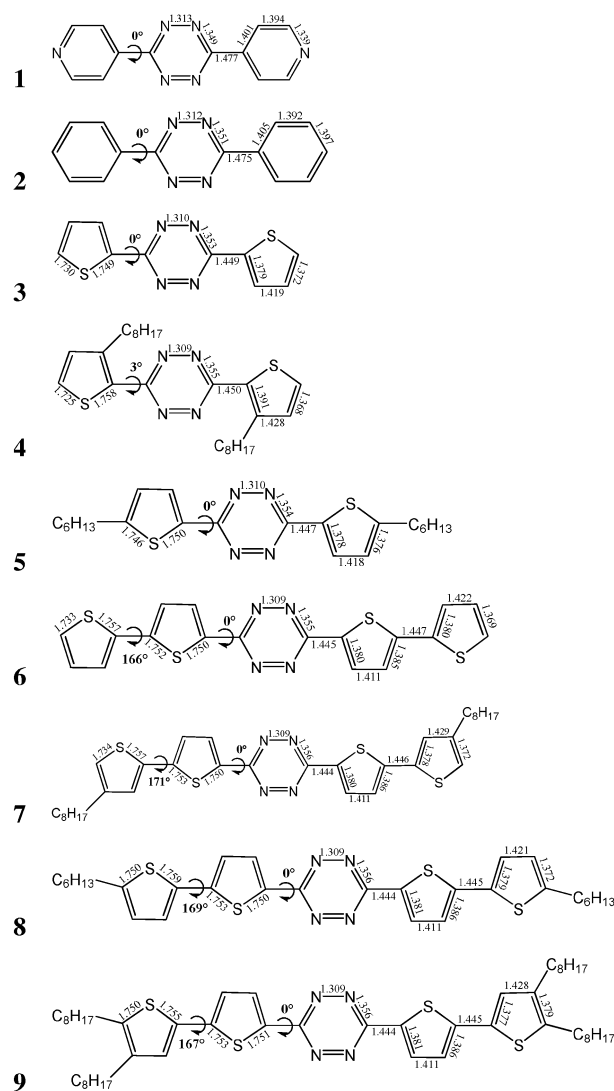


Fig. 1 Schematic structure of studied molecules, their optimal B3LYP/6-31G* bond lengths (in Å) and dihedral angles between the aromatic rings (in degrees).

Theoretical optimal structure

The presence of single bonds connecting the tetrazine unit with thiophene groups in the studied molecules leads to the formation of a large number of conformations. Based on the previous work of Liu *et al.*²⁶ we have restricted our calculations only to the symmetric all-*trans* conformations which exhibit the lowest total energies with respect to the steric conditions for oligothiophenes and related compounds.

The optimal B3LYP geometries for the non-substituted smallest molecules (three-ring compounds) (**1**, **2**, **3**) are totally planar. As presented in Fig. 1, the alkyl substitution in the inner C_β position is responsible for a small torsion of 3° calculated for **4**. The presence of two neighboring thiophene rings in the five-ring series leads to a certain torsion between them. The torsional angle in the non-substituted five-ring, **6**, is 166°. The effect of the thiophene ring connection with the tetrazine moiety on the geometry of the five-ring molecule can be estimated from the comparison of this dihedral angle with the corresponding angle in simple bithiophene. The calculated B3LYP/6-31G* torsion angle for bithiophene is 157°.²⁷ Subsequent DFT or *ab initio* MP2 quantum-chemical studies for this molecule^{28,29} report the energy minima for the *anti*-conformers at the torsion angles between 142° and 152°. It seems, therefore, that the presence of the central tetrazine ring is responsible for the lowering of the torsion angle between the neighboring thiophene rings. The theoretical calculations of other five-rings reveal that the planarity slightly increases upon substitution with alkyl groups. The torsion angle of 171° is found for **7** where the alkyl substituents in the terminal thiophene rings are located in the outer C_β position. The electron-donor effect of the alkyl substitution is thus reflected in the observed small dihedral angle changes (from 2 to 5°).

Although the molecules of the three-ring series contain substituents of different chemical nature (phenyl, pyridyl or thienyl), the mutual comparison of selected bonds is still quite interesting. As presented in Fig. 1, the N–N bond in the central

ring is the shortest (1.31 Å) whereas C–C bond linking the tetrazine central ring with the substituent is the longest. The value of 1.48 Å is found for **1** and **2** (phenyl and pyridine substituent), for **3** (thienyl substituent) this distance is 1.45 Å. The presence of alkyl groups in various positions of the thienyl substituent has different influence on the neighboring bonds. In general, shortening of the double bond is compensated by the elongation of the single bonds. The changes are within 10⁻² Å.

The aromaticity of studied molecules and its relation to their molecular structure can be described by the bond length alternation (BLA) parameter.^{27,30} This parameter might be defined as the averaged sum of the absolute values of the differences between the bond length (*d_i*) and the averaged bond length (\bar{d}):

$$\text{BLA} = \frac{\sum_{i=1}^M |d_i - \bar{d}|}{M} \quad (1)$$

In this definition, *M* stands for the number of aromatic bonds (*M* = 20 for **1** and **2** and *M* = 18 for **3** to **5** and *M* = 30 for **6** to **9**). With respect to this definition, a very small BLA value indicates effective aromatic structure, *e.g.* BLA of benzene is zero. The smallest BLA values of 0.038 and 0.030 were found for the optimal electronic ground state geometries of **1** and **2**, respectively (see Table 1). Three-ring compounds containing thienyl substituents show larger BLA values (from 0.125 to 0.128 Å). Elongation of the molecule by adding two thienyl rings (five-rings) leads to an increase of BLA by *ca.* 0.013 Å.

In this context it is interesting to comment the partial BLA* value for the hypothetical main conjugated backbone of the molecules studied. In this model, only the C–C, C–N and N–N bonds are accounted (see Fig. S1 in ESI†, *M* = 11 for **1** to **5** and *M* = 19 for **6** to **9**). The calculation results are also presented in Table 1 and they indicate the minimization of the bond length differences between the selected alternating

Table 1 The BLA values and the calculated B3LYP/6-31G* excitation energies (*E*). The second presented excitation energy was selected according to the dominant oscillator strength value (*f* > 0.6). The order of the excitation energy is indicated by the values written in *k*-column. Values written in italic and with asterisk symbol (*) stand for the BLA* of selected bonds (see Fig. S1 in ESI†)

Compound	BLA/Å	<i>k</i>	E/eV	Transition ^a	<i>k</i>	E/eV	<i>f</i>	Transition ^a
1	0.038 <i>0.043*</i>	1	2.15	H → L (86%)	12	4.23	0.9861	H – 3 → L + 1 (84%)
2	0.030 <i>0.033*</i>	1	2.24	H → L (86%)	7	3.97	1.0456	H – 1 → L + 1 (76%)
3	0.126 <i>0.034*</i>	1	2.23	H – 1 → L (86%)	4	3.51	0.8096	H → L + 1 (76%)
4	0.125 <i>0.036*</i>	1	2.18	H – 1 → L (85%)	4	3.41	0.6091	H → L + 1 (65%)
5	0.128 <i>0.033*</i>	1	2.23	H – 1 → L (86%)	4	3.34	1.1925	H → L + 1 (80%)
6	0.141 <i>0.031*</i>	1	2.24	H – 2 → L (80%)	3	2.68	1.6334	H → L + 1 (76%)
7	0.140 <i>0.034*</i>	1	2.24	H – 2 → L (84%)	3	2.65	1.7206	H → L + 1 (81%)
8	0.141 <i>0.030*</i>	1	2.24	H – 2 → L (86%)	3	2.57	1.8308	H → L + 1 (83%)
9	0.141 <i>0.032*</i>	1	2.24	H – 2 → L (84%)	3	2.54	1.9948	H → L + 1 (82%)

^a H stands for HOMO and L stands for LUMO. Values in parentheses represent the percentages of the excitation contributions to individual transitions.

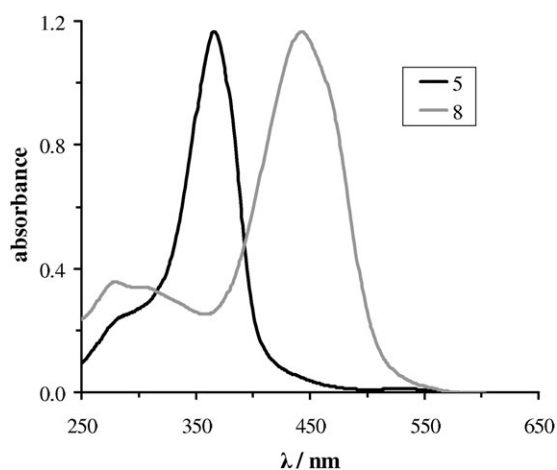


Fig. 2 UV-vis spectra of **5** and **8** recorded in CH_2Cl_2 .

single and double bonds with the increase of molecular size. Our calculations also show that not only the extension of the molecule length but also the addition of an alkyl substituents have an effect on the BLA* values calculated for the molecules studied.

Spectroscopic properties

The positions of UV-vis absorption bands of diaryltetrazines depend on the nature of the aryl rings, adjacent to the tetrazine ring and more particularly on their electron withdrawing/electron donating properties.²⁴ Representative spectra of the three-ring and five-ring series are shown in Fig. 2 whereas the UV-vis spectroscopic data for all compounds studied are collected in Table 2.

In all three-ring compounds the second band dominates the spectrum. In **1** and **2** this band is hypsochromically shifted with respect to the corresponding band in unsubstituted tetrazine, where it is located at 320 nm.³¹ This shift clearly manifests the electron withdrawing properties of the pyridyl substituent and, to a lesser extent, the phenyl one. In compounds with thienyl groups λ_{max} of the second band is located at higher wavelengths than in unsubstituted tetrazine due to electron donating properties of these substituents. In addition this band is strongly influenced by the presence of the alkyl substituent and its position in the thienyl ring. λ_{max} of the second band is bathochromically shifted for tetrazines with

alkylthienyl groups (**4** and **5**) as compared to the case of unsubstituted three-ring (**3**). Two factors inducing this bathochromic shift can be postulated: slightly increased electron donating effect of the alkylthienyl substituents as compared to non-substituted thienyl group and/or alkyl group induced planarization of the molecule. These suggestions are confirmed by the results of quantum chemical calculations (*vide infra*).

By comparison of the three-ring and the five-ring series it can be evoked that the conjugation length has the most pronounced effect on the position of the second band, which is bathochromically shifted in five-ring compounds by *ca.* 80–90 nm as compared to the corresponding three-ring ones (see spectra of **5** and **8** presented in Fig. 2). Again, as in the case of three-ring compounds, five-rings containing alkyl substituents (**7**, **8**, **9**) absorb at higher wavelengths than their unsubstituted analogue (**6**).

The first transition band, in the vicinity of 540 nm, clearly seen in compounds **1–5**, in **6** and **7** is present as a very weak shoulder. In **8**, **8a** and **9** it is not detectable. The position of this band is less dependent on the molecule length and the type of substituent, as typically found for this type of transition.³²

Based on the optimal B3LYP electronic ground state geometries, the fifteen TD-B3LYP vertical excitation energies were calculated (see Table S1, ESI†). For all studied molecules the first excitation energies has very low oscillator strength. The values collected in Table 1 show that the energies for three-ring molecules (**1** to **5**) are ranged from 2.15 to 2.24 eV. In the case of five-ring molecules (**6** to **9**), the position of the first excitation energy is 2.24 eV. The obtained results are in agreement with the experiment where, for the majority of cases, very weak and broad band or shoulders are detected in this energy region.

Comparing with the experiment, the optical transitions showing the dominant oscillator strength larger than 0.6 are connected with excitation energies of different order. It seems that the relevant highest excitation energies are connected with higher orders (see *k* values in Table 1). The energy of 4.23 eV obtained for **1** represents the twelfth transition. For the five-ring series (**6** to **9**) these energies are the third transitions. The theoretically calculated energy values are systematically lower than the experimental ones (the lowest shift of 0.05 eV was found for **5**, the highest of 0.26 eV for **6**). Nevertheless a simple linear relationship can be found between these

Table 2 Maxima of absorption bands (λ_{max}) measured in solution spectra (CH_2Cl_2 solvent) of diaryltetrazines studied in this research

Compound	First band/nm (eV)	Second band/nm (eV)	Third band/nm (eV)
1	545 vw ^a (2.28)	274 (4.43)	—
2	547 vw ^a (2.27)	298 (4.16)	—
3	531 vw ^a (2.34)	347 (3.57)	278 (4.46)
4	546 vw ^a (2.27)	353 (3.51)	266 (4.66)
5	534 vw ^a (2.32)	366 (3.39)	283 (4.38)
6	vws ^b	421 (2.94)	283 (4.38)
7	vws ^b	433 (2.86)	274 (4.52)
8	—	445 (2.79)	279 (4.44)
8a	—	443 (2.80)	276 (4.49)
9	—	455 (2.72)	278 (4.46)
			286 (4.34)

^a Very weak. ^b Very weak shoulder.

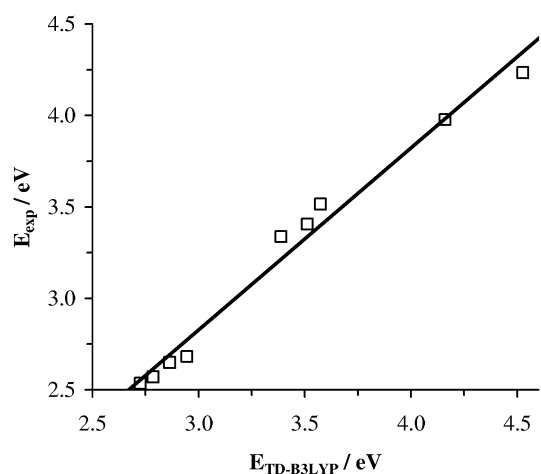


Fig. 3 Linear dependence between experimental and theoretical (TD-B3LYP/6-31G*) excitation energies with the first dominant oscillator strengths (second band).

results (see Fig. 3 and eqn (2)). The correlation coefficient of experimental energies (E_{exp}) vs. theoretical lowest excitation energies ($E_{TD-B3LYP}$) with the first dominant oscillator strength reached 0.991.

$$E_{exp} = 0.158 + 0.995 \times E_{TD-B3LYP} \text{ (eV)} \quad (2)$$

Based on the presented calculations and their correlation with the experimental results, the general effect of the alkyl group substitution on the absorption spectra of the molecules studied can be analyzed. First, the transition energies for the unsubstituted molecules are higher than those for the alkyl substituted ones. This is connected with a better planarity of the alkyl derivatives (see Fig. 1) as well as a slight increase of the electron donating properties of the thienyl groups caused by the presence of alkyl substituents. The strongest donating effect is predicted for **9**, where the excitation energy of 2.54 eV with largest oscillator strength was obtained (see Table 1).

To understand the physical background of the observed spectroscopic properties as well as to elucidate the electrochemical processes occurring in the synthesized molecules, it is useful to examine the shapes of the most important molecular orbitals. Since the shapes of these orbitals are only minimally affected by the substitution with the alkyl groups, the subsequent analysis will be presented only for the unsubstituted molecules. As shown in Table 1, the transition from the Highest Occupied to the Lowest Unoccupied Molecular Orbitals (HOMO-to-LUMO) contributes significantly to the first excitation energy only for compounds **1** and **2**. These contributions are practically constant (*ca.* 85%). The addition of thiophene rings to the tetrazine molecule is connected with the transition of (HOMO – 1)-to-LUMO for **3** to **5** and with (HOMO – 2)-to-LUMO for **6** to **9**. The HOMO orbitals for all studied molecules are uniformly delocalized only over the nitrogens of central tetrazine (see Fig. 4) and they are connected with the free electron pairs of these atoms. These orbitals have a typical non-bonding *n* character. The LUMO orbitals show the inter-ring bonding character and their lobes are uniformly spread along the tetrazine central ring and the neighbouring aryl groups. The (HOMO – 1) orbitals are

delocalized not only over the central tetrazine part, but electron clouds are shifted to the adjacent aryls, too. Their lobes are perpendicularly oriented to the aromatic chain. Both LUMO and (HOMO – 1) orbitals are of π -type. In the case of the optical transitions with the first dominant oscillator strength, the transitions to the (LUMO + 1) orbitals are important for all investigated molecules. As it can be seen in Fig. 4, this orbital is delocalised only over the tetrazine unit and the adjacent molecular units have minimal influence on this electron distribution. This orbital has an antibonding π type character. With respect to this analysis, the first optical transition (first band) for compounds **1** and **2** belongs to the n - π^* band. In the case of other molecules studied (**3** to **9**), the first optical transition has a clear π - π^* character. An interesting situation appears for optical transitions (second band) with the first dominant oscillator strength ($f > 0.6$). The contribution from HOMO-to-(LUMO + 1) is significant and therefore the n - π^* character of this transition is expected for thienyl molecules.

Electrochemical properties

Tetrazines substituted with thienyl or bithienyl substituents are electrochemically active showing a reversible redox couple at negative potentials and an irreversible oxidation peak at positive potentials with no signs of electropolymerization upon consecutive scans. The only exceptions are **6**, already described in the literature¹⁰ and **7** which undergo oxidative electrochemical polymerization upon potential scanning. A representative voltammogram for the series of tetrazine derivatives is shown in Fig. 5 whereas the electrochemical data determined for all compounds studied are collected in Table 3.

In a recent paper²⁴ redox behavior of various tetrazine derivatives were discussed with special emphasis on the correlation between the electron withdrawing/donating properties of the substituents and the standard potential of the reversible redox couple. According to the literature the standard potential of the reversible redox couple in unsubstituted tetrazine, E_1^0 , is –1.16 V vs. Fc/Fc⁺.³³ Among all compounds studied only in **1** a shift of E_1^0 towards higher potentials is observed ($E_1^0 = -1.12$ V) which can be treated as a manifestation of electron accepting properties of pyridyl substituents. The values of this potential, recorded for phenyl, thienyl and bithienyl derivatives of tetrazine, are consistently lower, indicating that they have a weakly electron donating effect on the central tetrazine ring. One can however notice a measurable effect of the presence the alkyl substituents on E_1^0 in the three-ring series. The unsubstituted compound **3** shows the highest value of E_1^0 , whereas in the case of **4**, in which the alkyl group is attached in the 4 position (inner β position) of the thienyl ring, this potential is lowered by 100 mV. An intermediate value of E_1^0 is found for **5** in which the alkyl substituent is located in the α position of the thienyl ring. The reduction process is little dependent on the conjugation length since the values of E_1^0 for **3** (unsubstituted three-ring compound) and **6** (unsubstituted five-ring compound) are very close. In the five-ring series the effect of the alkyl substituents is very weak and the values of E_1^0 are very close for all derivatives studied. This

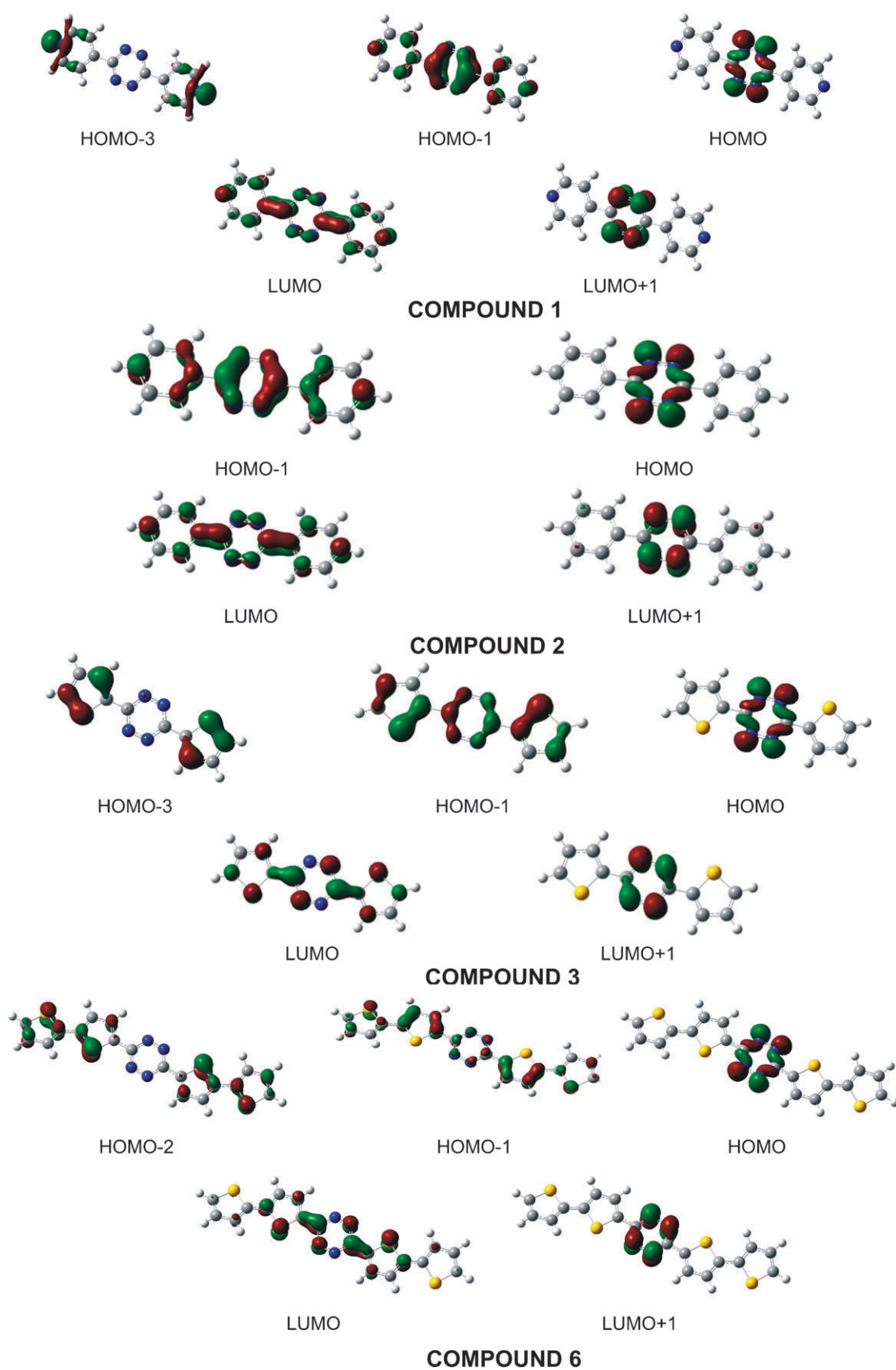


Fig. 4 Plots of B3LYP orbitals for unsubstituted molecules contributing to the selected excitation energies (see in Table 1).

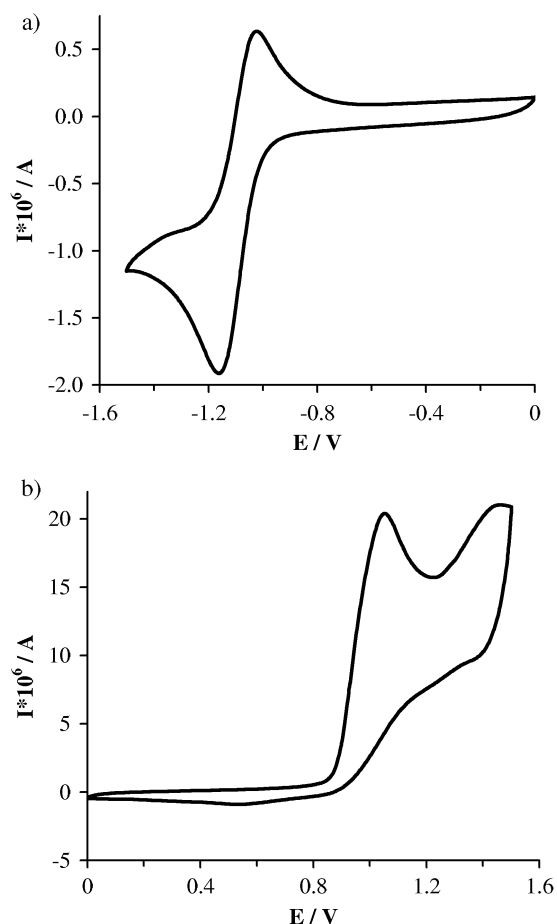


Fig. 5 Cyclic voltammogram of **8**; concentration 5×10^{-4} M; electrolyte 0.1 M Bu_4BF_4 in CH_2Cl_2 ; reference electrode Ag/Ag^+ ; scan rate 50 mV s^{-1} , (a) reduction part and (b) oxidation part.

Table 3 Oxidation and reduction potentials of diaryltetrazines determined from cyclic voltammetry investigations. Potential values are given with respect to the ferrocene couple (Fc/Fc^+), in V

Compound	Peak maximum		E_1^0	Peak onset	
	$E_{1\text{red}}$	$E_{1\text{ox}}$		$E_{1\text{red}}$	$E_{2\text{ox}}$
1	-1.17	-1.06	-1.12	-1.04	—
2	-1.39	-1.27	-1.33	-1.26	0.70
3	-1.30	-1.20	-1.25	-1.18	0.75
4	-1.44	-1.25	-1.35	-1.27	0.70
5	-1.43	-1.19	-1.31	-1.22	0.74
6	-1.28	-1.17	-1.23	-1.15	0.83
7	-1.28	-1.17	-1.23	-1.15	0.81
8	-1.32	-1.17	-1.25	-1.17	0.80
8a	-1.39	-1.20	-1.30	-1.22	0.79
9	-1.34	-1.17	-1.26	-1.18	0.74

is due to the presence of an unsubstituted spacer between the substituted thienyl ring and the tetrazine central unit. All these data seem to indicate that the reduction process essentially takes place in the central tetrazine unit. This is fully consistent with the DFT calculations.

As already stated oxidation of all compounds, occurring in the range of 0.7–0.8 V vs. Fc/Fc^+ , is irreversible and, with the exception of **6** and **7**, does not lead to electropolymerization. It is very little dependent on the nature of the substituent and the

Table 4 Calculated HOMO and LUMO levels and electrochemically determined LUMO levels, in eV

Compound	Experimental ^a LUMO	B3LYP/6-31G*	
		HOMO	LUMO
1	-3.76	-6.75	-3.19
2	-3.54	-6.17	-2.63
3	-3.62	-6.12	-2.65
4	-3.53	-5.94	-2.59
5	-3.58	-5.77	-2.45
6	-3.65	-5.46	-2.57
7	-3.65	-5.39	-2.52
8	-3.63	-5.25	-2.45
9	-3.62	-5.17	-2.41

^a Electrochemically determined.

molecule length since **2** (containing phenyl substituent) and **3** (containing thienyl substituent) start to oxidize at very similar potentials. The same applies to **3** and **6** which differ in their length. From the onsets of the first reduction peak, considering the absolute potential scale³⁴ the so called “electrochemical LUMO level” can be calculated according to eqn (3).³⁵

$$E_{\text{LUMO}} = -(E_{\text{red onset}} + 4.8) \text{ eV} \quad (3)$$

where $E_{\text{red onset}}$ denotes the onset of the first reduction peak (with respect to the Fc/Fc^+ couple, see column 5 in Table 3).

In Table 4 the electrochemically determined values of LUMO energies are compared with the calculated ones. It is instructive to compare the theoretically calculated LUMO levels with the electrochemically determined ones (see Table 4). First, we notice that with the exception of **1**, theoretical LUMO levels change very little within the whole series of the compounds studied. Similarly weak dependence of the nature the substituent and the length of the molecule on its LUMO level is observed in the electrochemical experiments. It should also be noted that the calculated LUMO levels are consistently higher by 0.9 to 1.2 eV with respect to the electrochemically determined ones. Finally, the experimental electrochemical results, together with the analysis of the frontier orbital shapes (see Fig. 4), indicate that the reduction process affects the whole molecule in the compounds of the three-ring series since the LUMO orbitals show the inter-ring bonding character and their lobes are uniformly spread along the tetrazine central ring and the neighbouring aryl rings. In the five-ring series the reduction process involves the increase of the electron density in the three core-rings whereas the two terminal ones are little affected. This explains the experimental observation of the weak dependence of the E_1^0 potential on the molecule length.

To the contrary, the lobes of the HOMO orbitals are localized on the tetrazine central ring (see Fig. 4), indicating that the oxidation process is initiated by abstraction of an electron from the tetrazine moiety. This observation is consistent with a weak dependence of the electrochemical oxidation peak onset on the nature of the aryl substituents.

Structural organization in the solid state

The preparation and the electroactive properties of **6** have already been reported,¹⁰ however its structure in the solid state has not yet been determined. We succeeded in preparing single

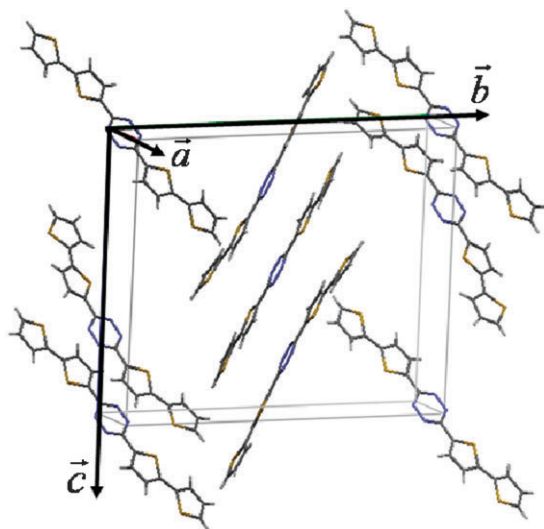


Fig. 6 Perspective view of the monoclinic unit cell found after refining the single crystal structure of **6**.

crystals of **6** suitable for refining its crystallographic structure. **6** crystallizes in a $P2_1/c$ space group, $Z = 4$ (one repeating unit is constituted of one molecular and a half entity), $a = 5.8286(2)$ Å, $b = 22.7537(9)$ Å, $c = 19.7775(7)$ Å and $\beta = 94.418(4)^\circ$ giving a density of $d = 1.564$ g cm $^{-3}$.† A perspective view of the unit cell is shown in Fig. 6. The molecular packing in the crystals of **6** is relatively complex. The molecules are paired and the formed pairs are stacked along two different types of columns. One column is oriented along a direction close to the c axis, while the stacking direction of the second one is close to a parallel of the (b,c) crystallographic plane. As a consequence, the molecular packets constituting these columns stay relatively apart from each other within the crystal structure. This structural arrangement does not favor the formation of an extended lattice of π - π

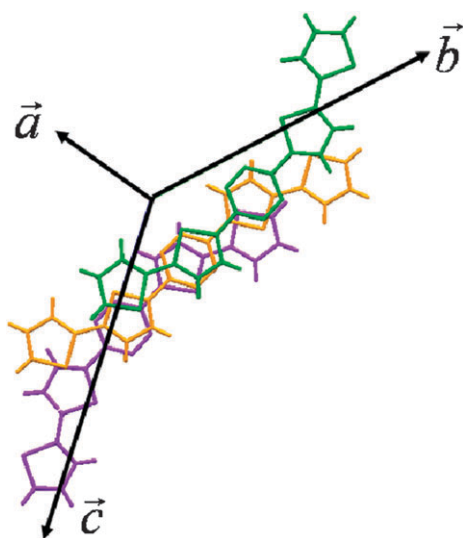


Fig. 7 Top view along the stacking axis of the molecular packets in columns showing details of the stacking mode of neighbouring molecules in which the shift from a face to face configuration can be clearly seen.

overlapping molecular orbitals which is believed to promote a high electronic delocalization. In Fig. 7 details of the stacking of three molecule packets constituting the second column are shown with a view along the stacking axis. The tetrazine rings are shifted and the deviation from a regular face-to-face stacking is measured to be equal to 57° . Moreover the terminal thienyl rings do not overlap at all in this stacking sequence. Finally the obtained intermolecular distances in this structural arrangement range from 3.52 Å for the shortest to 4.23 Å for the longest one, revealing some deviations from the full planar geometry of the molecules as can clearly be seen in Fig. 6. In the molecular crystallographic unit, deviations from the perfect planarity range in between 3.5° to 20° for thienyl and thienylene rings, respectively, to the perfect plane defined by the tetrazine ring. Concerning the torsional angles of thiophene rings, they range from 176.5° to 179.8° for the two extremes revealing that the molecular stacking in the solid state minimizes these values. This is in contrast with

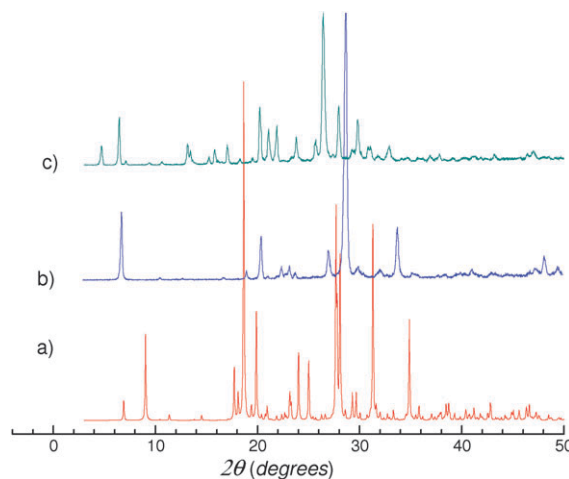


Fig. 8 X-Ray powder profiles of: (a) **6** calculated from the single crystal data, (b) **7** and (c) **9**.

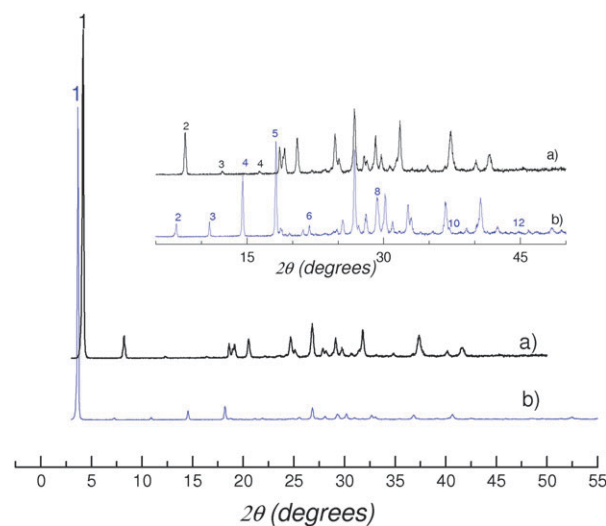


Fig. 9 X-Ray powder profiles of: (a) **8** and (b) **8a**. The inset is a zoom of the 5–50° 2θ range in which the Bragg peaks, possibly belonging to the same family as the most intensive one, are indexed accordingly.

the calculated values for the isolated molecules in which a 166° torsional angle is found for the terminal thienyl ring. (see **6** in Table 1).

For derivatives **7** to **9** only powder X-ray diffractograms could be measured. In Fig. 8 powder X-ray profiles of **6**, **7** and **9** are compared whereas in Fig. 9 the same profiles are shown for **8** and **8a**. It is clear that all powders studied are highly crystalline. Thus, the presence of alkyl terminal groups of different lengths and at different positions does not induce noticeable structural disorder since no increase of the diffuse background is observed in the recorded diffractograms. At this stage, it seems interesting to more clearly elucidate the structural arrangement of **7–9** by comparing their powder diffractograms with that of **6**, calculated from the single crystal data.

First, we can notice that the X-ray profiles of **7** and **9**, which contain octyl substituents in positions 4 and 4, 5, respectively, exhibit some similarities, suggesting probable structural relationships with **6** (see Fig. 8). For these compounds, the size of the unit cell does not seem larger than that determined for **6**. This indicates that, in spite of the presence of alkyl chains, the resulting molecular packing is probably denser than in **6**.

As expected, X-ray profiles of **8** and **8a** also show striking similarity (Fig. 9). A low angle Bragg peak, corresponding to a long distances of 24.7 \AA for **8** and 24.3 \AA for **8a**, shows the highest intensity in both cases. This indicates that the symmetry of the unit cells of these compounds, which differ only in the length of the alkyl substituent is certainly different from the symmetry of the unit cells of **6**, **7** and **9**. Moreover, this intensive low angle Bragg peak seems to be the first order of a family of Bragg reflections; higher order reflections of this family are indicated in the inset of Fig. 9. Since this distance corresponds to the length of the molecule, it can therefore be postulated that **8** and **8a** may exhibit a lamellar like structure, in which the molecules would stand upright in the lamellae. This structural arrangement is probably facilitated by the presence of terminal alkyl substituents in position 5 (outer C_α carbon).

To summarize this part of the research, it is clear from the X-ray diffraction studies that the supramolecular organization in the five-ring series is very dependent on the position of the substituent. In particular, the presence of the alkyl groups attached to C_α carbon in the terminal thienyl ring promotes the formation of a lamellar-type supramolecular organization.

Conclusions

To conclude, we have synthesized a series of solution processable diaryl tetrazine derivatives consisting of either three or five aromatic rings, the majority of them have never been reported. The synthesized compounds show tunable spectroscopic properties and interesting electrochemical behavior associated with a reversible reduction at relatively high potentials and an irreversible oxidation. The solid state structure of the synthesized five-ring compounds is very sensitive to the position of the solubilizing alkyl substituents. It has been shown that substituents attached to C_α carbon in the terminal

thienyl ring induce the formation of a lamellar-type supramolecular organization.

The obtained experimental results have been correlated with those derived from quantum chemical calculations. In particular, the B3LYP calculations have shown that the presence of the tetrazine central unit is responsible for the lowering of the torsion angle between the adjacent aromatic rings which leads to planarisation of the whole molecule. This point is strongly confirmed by the analysis of X-ray data obtained for single crystals of **6**. The studied molecules also exhibit different bond length alternation (BLA) parameters. Although the largest molecules (**6** to **9**) have the highest BLA values, the minimization of bond length differences between the selected single and double bonds within the main conjugation chain has been found. The calculated optical transitions with the dominant oscillator strengths show very good linear relationship with the relevant experimental values. The presented orbital analysis has also revealed that the contribution from HOMO-to-(LUMO + 1) is for thienyl tetrazines significant and the $n-\pi^*$ for character of this transition is expected. The investigation of the shapes of frontier orbitals showed that the oxidation of tetrazine derivatives is connected with the electron abstraction from the tetrazine moieties. To the contrary, the electrochemical reduction leads to the increase of electron density in bonds linking tetrazine with adjacent rings. The results obtained from quantum chemical calculations are fully consistent with experimental findings.

Acknowledgements

Financial support from Polish Ministry of Science and Higher Education through research project no. NN205105735 in years 2008–2011 is acknowledged.

References

- 1 A. R. Murphy and J. M. J. Frechet, *Chem. Rev.*, 2007, **107**, 1066.
- 2 S. Allard, M. Forster, B. Souharce, H. Thiem and U. Scherf, *Angew. Chem., Int. Ed.*, 2008, **47**, 4070.
- 3 T. Rauch, M. Böberl, S. F. Tedde, J. Fürst, M. V. Kovalenko, G. Hesser, U. Lemmer, W. Heiss and O. Hayden, *Nat. Photonics*, 2009, **3**, 332.
- 4 U. Lange, N. V. Roznyatovskaya and V. M. Mirsky, *Anal. Chim. Acta*, 2008, **614**, 1.
- 5 M.-J. Spijckman, J. J. Brondijk, T. C. T. Geuns, E. C. P. Smits, T. Cramer, F. Zerbetto, P. Stoliar, F. Biscarini, P. W. M. Blom and D. M. de Leeuw, *Adv. Funct. Mater.*, 2010, **20**, 898.
- 6 A. Malinauskas, J. Malinauskiene and A. Ramanavicius, *Nanotechnology*, 2005, **16**, R51.
- 7 Y. J. Cheng, S. H. Yang and C. S. Hsu, *Chem. Rev.*, 2009, **109**, 5868.
- 8 A. Pron, P. Gawrys, M. Zagorska, D. Djurado and R. Demadrille, *Chem. Soc. Rev.*, 2010, **9**, 2577.
- 9 J. Soloducho, J. Doskocz, J. Cabaj and S. Roszak, *Tetrahedron*, 2003, **59**, 4761.
- 10 P. Audebert, S. Sadki, F. Miomandre and G. Clavier, *Electrochem. Commun.*, 2004, **6**, 144.
- 11 G. Barbarella, P. Ostoja, P. Maccagnani, O. Pudova, L. Antolini, D. Casarini and A. Bongini, *Chem. Mater.*, 1998, **10**, 3683.
- 12 Y. Kim, J. Do, E. Kim, G. Clavier, L. Galmiche and P. Audebert, *J. Electroanal. Chem.*, 2009, **632**, 201.
- 13 N. Saracoglu, *Tetrahedron*, 2007, **63**, 4199.
- 14 G. Clavier and P. Audebert, *Chem. Rev.*, 2010, **110**, 3299.
- 15 I. Osaka and R. D. McCullough, *Acc. Chem. Res.*, 2008, **41**, 1202.

- 16 It is instructive to compare the strikingly different optical and redox properties of regioregular ht–ht coupled poly(alkylthiophene)s, first synthesized by (a) T. A. Chen and R. D. Rieke, *J. Am. Chem. Soc.*, 1992, **114**, 10087; (b) R. R. McCullough and R. D. Lowe, *J. Chem. Soc., Chem. Commun.*, 1992, 70 with hh–tt or tt–hh coupled poly(alkylthiophene)s synthesized by; (c) M. Zagorska and B. Krische, *Polymer*, 1990, **31**, 1379; (d) R. M. Souto-Maior, K. Hinkelmann, H. Eckert and F. Wudl, *Macromolecules*, 1990, **23**, 1268.
- 17 T. J. Prosa, M. J. Winokur, J. Moulton, P. Smith and A. J. Heeger, *Macromolecules*, 1992, **25**, 4364.
- 18 R. G. Parr and W. Yang, *Density-Functional Theory of Atoms and Molecules in Chemistry*, Springer-Verlag, New York, 1991.
- 19 A. D. Becke, *J. Chem. Phys.*, 1993, **98**, 5648.
- 20 F. Furche and R. Ahlrichs, *J. Chem. Phys.*, 2002, **117**, 7433.
- 21 G. A. Petersson and M. A. Al-Laham, *J. Chem. Phys.*, 1991, **94**, 6081.
- 22 V. Rassolov, *J. Comput. Chem.*, 2001, **22**, 976.
- 23 M. J. Frisch, G. W. Trucks, H. B. Schlegel, G. E. Scuseria, M. A. Robb, J. R. Cheeseman, J. A. Montgomery, Jr., T. Vreven, K. N. Kudin, J. C. Burant, J. M. Millam, S. S. Iyengar, J. Tomasi, V. Barone, B. Mennucci, M. Cossi, G. Scalmani, N. Rega, G. A. Petersson, H. Nakatsuji, M. Hada, M. Ehara, K. Toyota, R. Fukuda, J. Hasegawa, M. Ishida, T. Nakajima, Y. Honda, O. Kitao, H. Nakai, M. Klene, X. Li, J. E. Knox, H. P. Hratchian, J. B. Cross, C. Adamo, J. Jaramillo, R. Gomperts, R. E. Stratmann, O. Yazyev, A. J. Austin, R. Cammi, C. Pomelli, J. W. Ochterski, P. Y. Ayala, K. Morokuma, G. A. Voth, P. Salvador, J. J. Dannenberg, V. G. Zakrzewski, S. Dapprich, A. D. Daniels, M. C. Strain, O. Farkas, D. K. Malick, A. D. Rabuck, J. B. Raghavachari, J. V. Foresman, Q. Ortiz, A. G. Cui, S. Baboul, J. Clifford, B. B. Cioslowski, K. Stefanov, G. Liu, A. Liashenko, P. Piskorz, I. Komaromi, R. L. Martin, D. J. Fox, T. Keith, M. A. Al-Laham, C. Y. Peng, A. Nanayakkara, M. Challacombe, P. M. W. Gill, B. Johnson, W. Chen, M. W. Wong, C. Gonzalez and J. A. Pople, *GAUSSIAN 03, Revision A.1*, Gaussian, Inc., Pittsburgh, PA, 2003.
- 24 Y.-H. Gong, F. Miomandre, R. Méallet-Renault, S. Badre, L. Galmiche, J. Tang, P. Audebert and G. Clavier, *Eur. J. Org. Chem.*, 2009, 6121.
- 25 M. Wlostowski and A. Olszewski, in preparation.
- 26 F. Liu, P. Zuo, L. Meng and S. J. Zheng, *THEOCHEM*, 2005, **726**, 161.
- 27 V. Lukeš, R. Šolc, J. Rimarčák, S. Guillerez and B. Pépin-Donat, *THEOCHEM*, 2009, **910**, 104.
- 28 S. M. Bouzzine, S. Bouzakraoui, M. Bouachrine and M. Hamidi, *THEOCHEM*, 2005, **726**, 271.
- 29 W. J. D. Beenken, *Chem. Phys.*, 2008, **349**, 250.
- 30 D. Jacquemin, E. A. Perpète, H. Chermette, I. Ciofini and C. Adamo, *Chem. Phys.*, 2007, **332**, 79.
- 31 A. R. Katritzky, *Handbook of Heterocyclic Chemistry*, Pergamon Press, Oxford, 1986.
- 32 J. Wałuk, J. Spanget-Larsen and E. W. Thulstrup, *Chem. Phys.*, 1995, **200**, 201.
- 33 H. Fischer, T. Müller, I. Umminger, F. A. Neugebauer, H. Chandra and M. C. R. Symons, *J. Chem. Soc., Perkin Trans. 2*, 1988, 413.
- 34 S. Trasatti, *Pure Appl. Chem.*, 1986, **58**, 955.
- 35 T. Johansson, W. Mammo, M. Svensson, M. R. Andersson and O. Inganäs, *J. Mater. Chem.*, 2003, **13**, 1316.